

Conductance stability and Na⁺ interaction with Shab K⁺ channels under low K⁺ conditions

Froylán Gómez-Lagunas, Elisa Carrillo, and Carolina Barriga-Montoya

School of Medicine, Department of Physiology, National Autonomous University of Mexico (Unam), México City, México

ABSTRACT

K⁺ ions exert a structural effect that brings stability to K⁺ selective pores. Thus, upon bathing Shab channels in 0 K⁺ solutions the ion conductance, G_K, irreversibly collapses. Related to this, studies with isolated KcsA channels have suggested that there is a transition [K⁺] around which the pore takes one of two conformations, either the low (non-conducting) or high K⁺ (conducting) crystal structures. We examined this premise by looking at the K⁺-dependency of G_K stability of Shab channels within the cell membrane environment. We found that: K⁺ effect on G_K stability is highly asymmetrical, and that as internal K⁺ is replaced by Na⁺ G_K drops in a way that suggests a transition internal [K⁺]. Additionally, we found that external permeant ions inhibit G_K drop with a potency that differs from the global selectivity-sequence of K⁺ pores; the non-permeant TEA inhibited G_K drop in a K⁺-dependent manner. Upon lowering internal [K⁺] we observed an influx of Na⁺ at negative potentials. Na⁺ influx was halted by physiological external [K⁺], which also restored G_K stability. Hyperpolarized potentials afforded G_K stability but, as expected, do not restore G_K selectivity. For completeness, Na⁺ interaction with Shab was also assessed at depolarized potentials by looking at Na block followed by permeation (pore unblock) at positive potentials, in solutions approaching the 0 K⁺ limit. The stabilizing effect of negative potentials along with the non-parallel variation of Na⁺ permeability and conductance-stability herein reported, show that pore stability and selectivity, although related, are not strictly coupled.

ARTICLE HISTORY

Received 29 July 2021
Revised 24 September 2021
Accepted 9 October 2021



KEYWORDS

Potassium channels; hypokalemia; conductance stability; selectivity; TEA blockage; Na blockage

Introduction

In addition to permeate through potassium channels K⁺ ions keep stable the pore conformation capable to conduct ions. Evidence of this central property of K⁺ channels came first from electrophysiological studies carried out on voltage-gated channels. Studying the squid K channel Almers & Armstrong [1] noticed that K channel activity gradually vanishes upon K⁺ removal from the recording solutions. A similar phenomenon was afterward observed in Shaker channels [2]. It was found that, in contrast to the squid channel, the Shaker K⁺ conductance (G_K) remains unchanged upon exposure to 0 K⁺ solutions, as long as the channels are kept undisturbed, closed, while they are bathed in 0 K⁺, however if they are gated, with the delivery of depolarizing pulses, then G_K collapses. In the case of Shaker, G_K drop does not depend on the frequency of pulsing in 0 K⁺, and is fully reversed by

prolonged depolarizations, which demonstrates that the drop of G_K is not due to inactivation [2]. Shab responds to immersion in 0 K⁺ solutions in a manner similar to that of the squid K⁺ channel, namely: Shab G_K drops passively (i.e., with the channels kept closed at the resting potential) during channel exposure to 0 K⁺, and the drop of G_K is irreversible [1,3]. In both Shab and Shaker channels, Na⁺ replacement with the bigger and impermeant choline or NMG ions slows down G_K collapse in 0 K⁺, although interestingly, this effect is more pronounced in Shaker than in Shab [3–5]. Na⁺ substitution by Cs⁺, in the absence of K⁺, also maintains the Shab conductance stable [6]. These observations indicate that Na⁺ ions somehow catalyze G_K collapse in the absence of K⁺. G_K collapse in 0 K⁺ is voltage dependent, hyperpolarized holding potentials inhibit G_K drop of both Shaker and Shab channels [2,5,7,8]. The latter shows that the membrane

CONTACT Froylán Gómez-Lagunas  froylangl@yahoo.com  School of Medicine, Department of Physiology, National Autonomous University of Mexico (Unam), México City, México

© 2021 The Author(s). Published by Informa UK Limited, trading as Taylor & Francis Group.
This is an Open Access article distributed under the terms of the Creative Commons Attribution License (<http://creativecommons.org/licenses/by/4.0/>), which permits unrestricted use, distribution, and reproduction in any medium, provided the original work is properly cited.

potential has a relevant role on the K^+ -dependent G_K stability, one that cannot be assessed by crystal structures nor biochemical studies carried out with purified, membrane-devoid, proteins. Regarding the structural framework of the above observations, the known landmark studies of MacKinnon's lab [9], have shown that K^+ channel pores present 4 K^+ binding sites (named s1 to s4, from outside to inside) placed in series and at regular distances, along the narrow (3 Å radius x 12 Å long) and extracellularly oriented region of the pore known as the selectivity filter (SF), which contains the amino-acid signature sequence of K^+ channels (TVGYG) [9,10]. Oxygens of main-chain carbonyls of signature sequence amino acids, along with that of the hydroxyl side-chain of the s4 threonine, point toward the pore lumen, forming 4 cages of 8 oxygens each, that coordinate a centrally located K^+ ion (radius = 1.3 Å). In the zero-voltage crystals, K^+ ions are located at every third position, with an s1-s3 occupancy being as likely as an s2-s4 K^+ occupancy. With the cytoplasmic gate closed, an additional K^+ ion is seen at the center of the region known as the central cavity of the pore [9]. The above, capable to conduct K^+ ions structure, is obtained with high $[K^+]$ crystallization solutions (200 mM), and hence it is referred to as the high K^+ structure, to contrast it against a KcsA structure observed with low K^+ crystallization solutions (5 mM), named the low K^+ structure [11]. The latter, presents a distorted pore structure, considered unlikely to conduct K^+ , in which the SF harbors a single K^+ ion, located at either s1 or s4, since the SF valine and glycine residues have a distorted orientation, which eliminates the central s2 & s3 positions as K^+ binding sites. Related to this, and interestingly, it has been proposed that there is a transition $[K^+]$, around which the pore falls into either the low or high- K^+ conformations [12–14]. On the other hand, in spite of the mentioned physiological and crystallographic observations, not all K^+ -selective channels seem to require K^+ ions to remain functional. For example, it has been reported that delayed rectifier channels of frog sympathetic neurons [15], as well as Kv2.1 channels of cervical ganglia [16] remain active upon K^+ removal, although allowing the anomalous passage of Na^+ ions. Further work is clearly needed to determine the K^+ requirements of the K^+ channel family.

Herein, we extend our former observations on the K^+ -dependent stability of K^+ channels. We

gradually replaced K^+ with Na^+ ions, and observed the effect of this manipulation in stability, selectivity, and Na^+ block of Shab G_K . Among other observations we report that, with channels within the cell membrane environment, as internal $[K^+]$ decreases G_K drops in a way consistent with the presence of a transition $[K^+]$, around which the pore either falls relatively fast into an irreversible non-conducting state, or remains comparatively longer in a capable to conduct, although less selective, conformation; in qualitative agreement with studies carried out with isolated KcsA channels. Additionally, we found that along with G_K destabilization, hypokalemic (non-zero K^+) solutions allow Na^+ permeation at negative voltages. Hyperpolarized holding potentials keep channel conductance stable under these conditions [7] but, as expected, they do not restore pore selectivity. On the other hand, at depolarized potentials we found that Na^+ interaction with the channels (i.e., internal Na^+ block with solutions that approach the 0 K^+ limit) becomes apparent from negative potentials, and presents a blockage electrical-distance near one. The differential role of the membrane voltage on stability and selectivity, along with the non-parallel variation of G_K stability and Na^+ permeability herein reported, support the notion that: pore stability and selectivity, although clearly related [e.g., 6, 8, 17, 18, this work] are not strictly coupled parameters.

Materials and methods

Cell culture and Shab channel expression

Insect Sf9 cells were grown at 27°C in Ex-Cell 420 medium (Sigma) containing an added 10% fetal bovine serum (Sigma). Cells were infected with a recombinant baculovirus containing Shab K-channel cDNA (dShab 11, Gene Bank Accession Number M32659.1) [17, 18] with a multiplicity of infection ~10. Experiments were conducted 48 h after infection, as reported [7].

Electrophysiological recordings

Macroscopic currents were recorded under whole-cell patch clamp, with an Axopatch 1D amplifier (Axon Instruments). Currents were filtered on-line and sampled at rates that fulfilled the Nyquist

criteria, with a Digidata 1322A interface (Axon Instruments). Electrodes were made of borosilicate glass (KIMAX 51) pulled to a 1–1.5 M Ω resistance, 80% of series resistance was compensated, as reported [7].

Solutions

Solutions will be named by their main active, test, cation and location across the membrane. External solutions contained (mM): Na_o (0 K_o): 145 NaCl, 10 CaCl₂, 10 HEPES-NaOH. XK_o: X KCl, 145-X NaCl, 10 CaCl₂, 10 HEPES-NaOH. Internal solutions contained (mM): K_i: 30 KCl, 90 KF, 2 MgCl₂, 10 EGTA-KOH, 10 HEPES-KOH; Na_i: 30 NaCl, 90 NaF, 2 MgCl₂, 10 EGTA-NaOH, 10 HEPES-NaOH. X_{Ki} solutions were prepared by mixing K_i and Na_i solutions to yield the desired [K⁺]_i, keeping the molar fractions X_{Ki}+X_{Na_i} = 1. pH of all solutions was 7.2. Solutions were changed using a gravity driven perfusion system, as reported [7]. With a recoding chamber volume of 250 μ L, full exchange of solutions took < 10 sec. Junction potentials estimated following standard procedures, as reported [6,19], were smaller than \pm 3 mV.

Data analysis

Currents were analyzed with Clampfit (Axon Instruments). Curve fitting was carried out with SigmaPlot 10.6 & GraphPad Prism 5 (GraphPad software). Statistical analysis was done with GraphPad Prism 5. Points are mean \pm SEM of at least 4 independent experiments. Significance level was set at 0.05.

Results

For a reference, a typical experiment that illustrates the irreversible loss of K⁺ conductance, G_K, upon channels exposure to 0 K⁺ solutions is presented in (Figure 1(a)). The experiment was carried out using a 30 mM [K_o⁺] control solution (see Methods), a concentration which is near the hemolymph [K⁺] concentration of *Drosophila* (36–55 mM) [20], the organism from which Shab DNA was cloned [17], and that, more importantly, affords stability to Shab G_K (see below). To test G_K

stability, control K⁺ current (Figure 1(a) left panel) is recorded by applying activating pulses (0 mV/30 ms from the HP of –80 mV), with the cell bathed in solutions where G_K is stable (30 K_o/Na_i, see Methods). Thereafter, the cell is superfused with the test, Na⁺-containing, external solution lacking K⁺ (Na_o/Na_i condition) for a variable time (5 min in the case illustrated), with the channels kept closed at the HP (indicated by the arrow). Finally, the cell is superfused back with 30 mM [K_o] solution, and the state of the channels is tested. The trace in the right panel illustrates that a 5 min exposure to 0 K⁺ eliminates G_K almost completely. GK stability is assessed from experiments as in A by the ratio I(t)/I_o (Figure 1(b)), where I(t) is I_K amplitude left after t-min exposure of channels to 0 K⁺, and I_o is the control (t = 0) current amplitude (data from [7], see Figure Legend).

We had previously stated that external K⁺ was slightly more effective at keeping G_K stable than internal K⁺. However, this was observed comparing the effect of high [K⁺] solutions, which already kept G_K rather, and comparably, stable (120 mM K_i vs. 100 mM K_o) [3]. Since the sidedness of K⁺ effect on G_K has a clear relevance to K⁺ channels functioning, we reviewed our previous statement by testing the relative effectiveness of lower, nearly symmetric, [K⁺] across the membrane. The latter is presented in (Figure 1(c)) which shows G_K stability as a function of the time of whole-cell recording, with channels bathed in either 30K_o/Na_i (as the control in A, open circles) or Na_o/35 K_i solutions (closed circles, see Figure legend). Note that, G_K is notably more stable with K⁺ present in only the external solution (see later & Discussion).

G_K stability under low [K⁺] conditions. A test for a transition [K_i⁺]

Studies with purified KcsA proteins have suggested that there is a transition [K⁺] around which the pore takes either the low or the high-K⁺ crystal structures that have been observed in this channel (Introduction). As these studies are done with isolated proteins, we were interested in determining whether in the cell membrane environment there was also evidence of

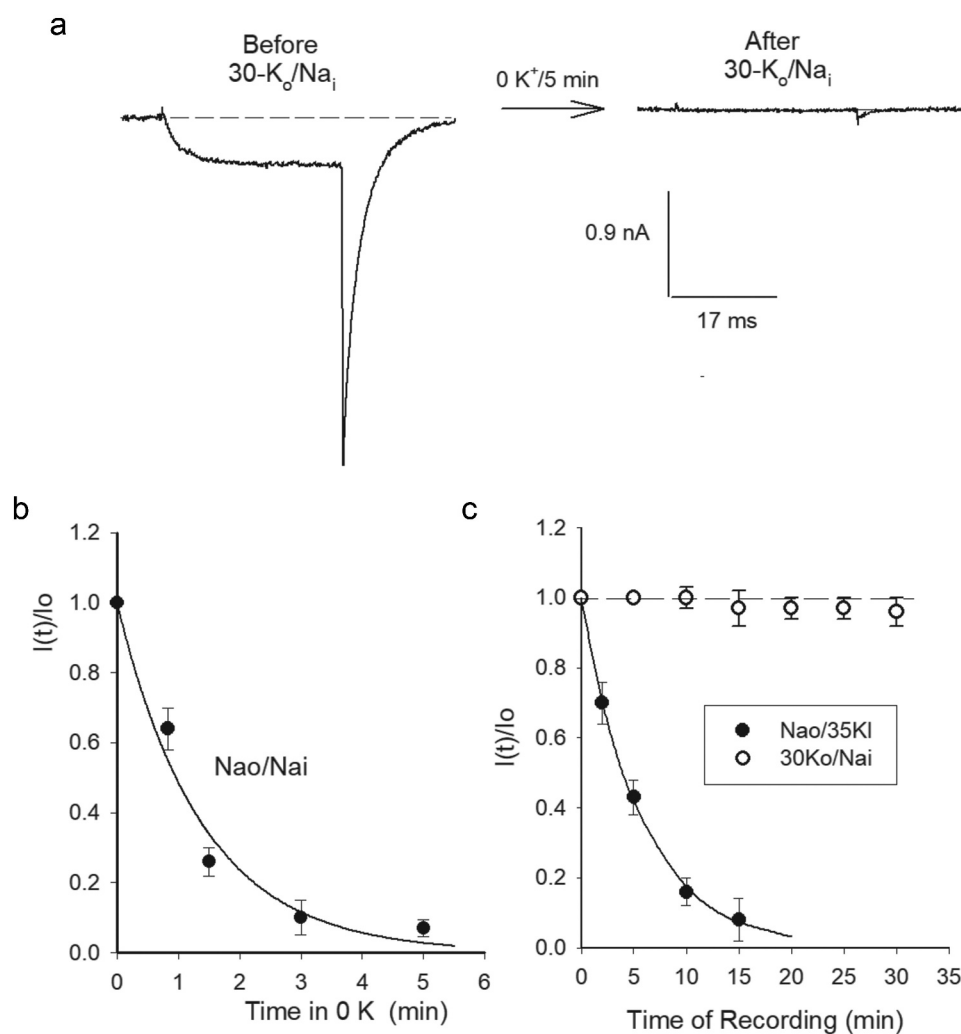


Figure 1. G_K drop in hypokalemic solutions. (a) Left panel, Control I_K evoked by a 0 mV/30 ms pulse with the cell bathed in 30K_o/Na_i solutions. HP = -80 mV. Right panel, I_K left after exposing the cell to 0 K⁺ (Na_o/Na_i) solutions across the membrane for 5 min (see Text), while V_m was kept constant at the HP. (b) $I(t)/I(0)$ vs. Time in 0 K⁺, $I(t)$ is I_K left after exposing the cell for t-min to 0 K⁺, I_0 is the initial, control, I_K as in A. The line is the fit of the points with a single exponential function $I(t)/I(0) = \exp(-t/\tau)$, with $\tau = 1.4$ min. (c) G_K stability assessed as $I(t)/I(0)$ vs. Time of whole-cell recording. I_K was measured applying 0 mV/30 ms activating pulses at the indicated times, $V_m = -80$ mV between pulses. Cells were bathed in either Na_o/35K_i (closed circles) or 30K_o/Na_i (open circles) solutions. The solid line is the fit of the points (Na_o/35K_i) with a single exponential function with $\tau = 5.7$ min, as in B. A&B were taken from Gomez-Lagunas, 2007 [7].

a corresponding transition $[K_i]$, around which the pore would either fall relatively fast into an irreversible non-conducting state, or remain comparatively longer in a functional conformation.

To test the above, G_K stability was assessed in the absence of external K⁺, following the time course of I_K amplitude in cells dialyzed with, Na⁺-containing, internal solutions having a variable $[K_i^+]$ (with $X_{KI} + X_{NaI} = 1$, where X stands for molar fraction, see Methods), as in (Figure 1(c)). Figure 2a shows G_K stability ($I(t)/I_0$ ratio) plotted against time of whole-cell recording, at the indicated $[K_i^+]$. Note that, as expected, G_K stability

drops as internal $[K^+]$ decreases and, more interestingly, note that the data clusters into two groups, with markedly different rate of G_K drop, one corresponding to $[K_i^+] \leq 47$ mM, and the other to $[K_i^+] \geq 60$ mM. We interpret this observation as suggestive of a transition $[K_i^+]$, located somewhere between 47 and 60 mM, at -80 mV. The latter is more clearly noticed in (Figure 2(b)) which presents the plot of the initial slope of the points in A vs. $[K_i^+]$ (see Figure legend). Note the abrupt change in the slopes trend. The dashed lines through the points serve to enhance the markedly different trend of the slopes, and lack any physical

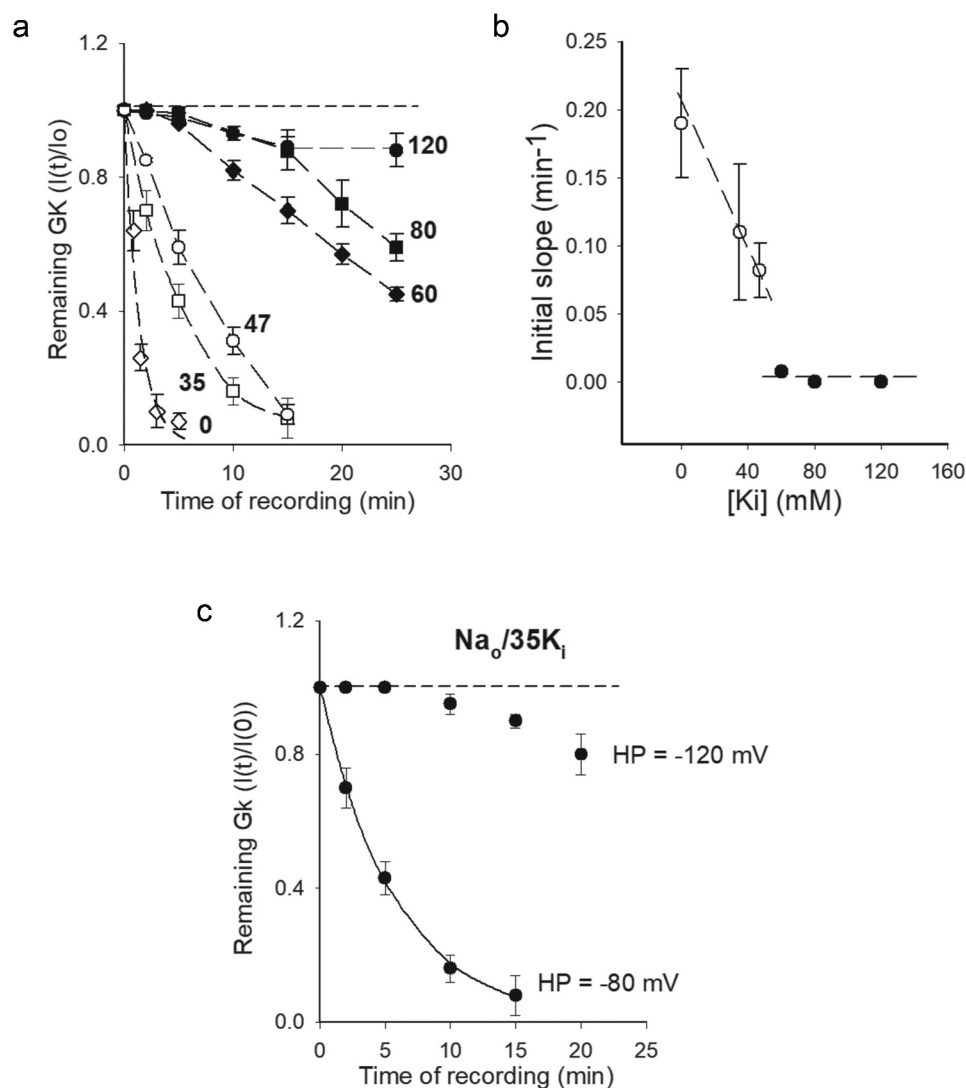


Figure 2. G_K stability vs. $[K_i]$. (a) Remaining G_K ($I(t)/I_0$) vs Time of recording, as in Figure 1c. Cells were bathed in Na^+ -containing internal solutions containing the indicated $[K_i]$ (with $X_{K_i} + X_{\text{Na}_i} = 1$, see text). External solution was Na_o . Note that the data clusters into two sets. (b) Initial slope vs. $[K_i]$. Initial slope was assessed as the slope of the straight line that connects the first two points in A ($I(t = 0)$) with the next $I(t \approx 2 \text{ min})$ point. The dashed lines have no physical meaning, they serve to best point out the data division into two sets. (c) G_K stability of channels bathed in $\text{Na}_o/35\text{K}_i$ solutions at the HP of either -80 or -120 mV, as indicated.

meaning (see (Figure (6)) of Zhou & Mackinnon, 2003 [14]). The above observations qualitatively agree with the studies done with purified KcsA channels [11–14], suggesting that similar K^+ -dependent structural changes may occur in the pore of voltage-dependent channels within the cell membrane environment, although in the latter G_K stability is voltage-dependent (see below & Discussion).

Figure 2(c) shows, that similar to the case of 0 K^+ across the membrane [7], a hyperpolarized HP (-120 mV) stabilizes G_K in hypokalemic, non- 0 K^+ , conditions. This shows that even millimolar

amounts of internal K^+ do not bypass the stabilizing role exerted by negative V_m .

Inhibition of G_K drop by external monovalent cations

Thereafter, we studied the effect of externally added cations on G_K stability. Our goal was to determine whether the potency with which different ions may prevent G_K collapse correlated with the global selectivity-sequence of K^+ pores.

Figure 3(a) illustrates I_K recorded in $30\text{K}_o/\text{Na}_i$ solutions before and after bathing the cells for

5-min with the indicated test cation, Na^+ -containing, external solutions ([test cation] = 5 mM), while V_m was kept constant at the HP of -80 mV, as in (Figure 1(a)). The observations, summarized in (Figure 3(b)), show that monovalent cations prevent G_K drop with a potency that follows the sequence: $\text{Na}^+ < \text{NH}_4^+ < \text{Cs}^+ < \text{Rb}^+ \approx \text{K}^+$. The latter differs from the global selectivity-sequence of K channels, in which NH_4^+ is more permeable than Cs^+ . This suggests the simplest hypothesis that the order in (Figure 3(b)) could correspond to the selectivity of a particular, externally accessible, pore site which upon occupancy by a suitable cation keeps G_K stable. Regarding the test cation concentration in

(Figure 3(a)) (5 mM), it is interesting to note that although the *Drosophila* hemolymph presents an elevated $[\text{K}^+]$, due to its blood-brain barrier a much lower 5 mM $[\text{Ko}^+]$ baths brain cells [20], similar to the external $[\text{Ko}^+]$ of mammalian cells. Considering the observations in (Figure 3), and that the non-permeant TEA cation inhibits G_K drop of Shaker acting from the external side of the membrane [2], we seek to determine whether external TEA would also inhibit Shab G_K drop. To do this, firstly we determined the basic parameters of TEA_o block of Shab, namely the voltage dependence of its apparent affinity, which as far as we know has not been reported yet. The traces in (Figure 4(a)) indicate that ~80% of channels are

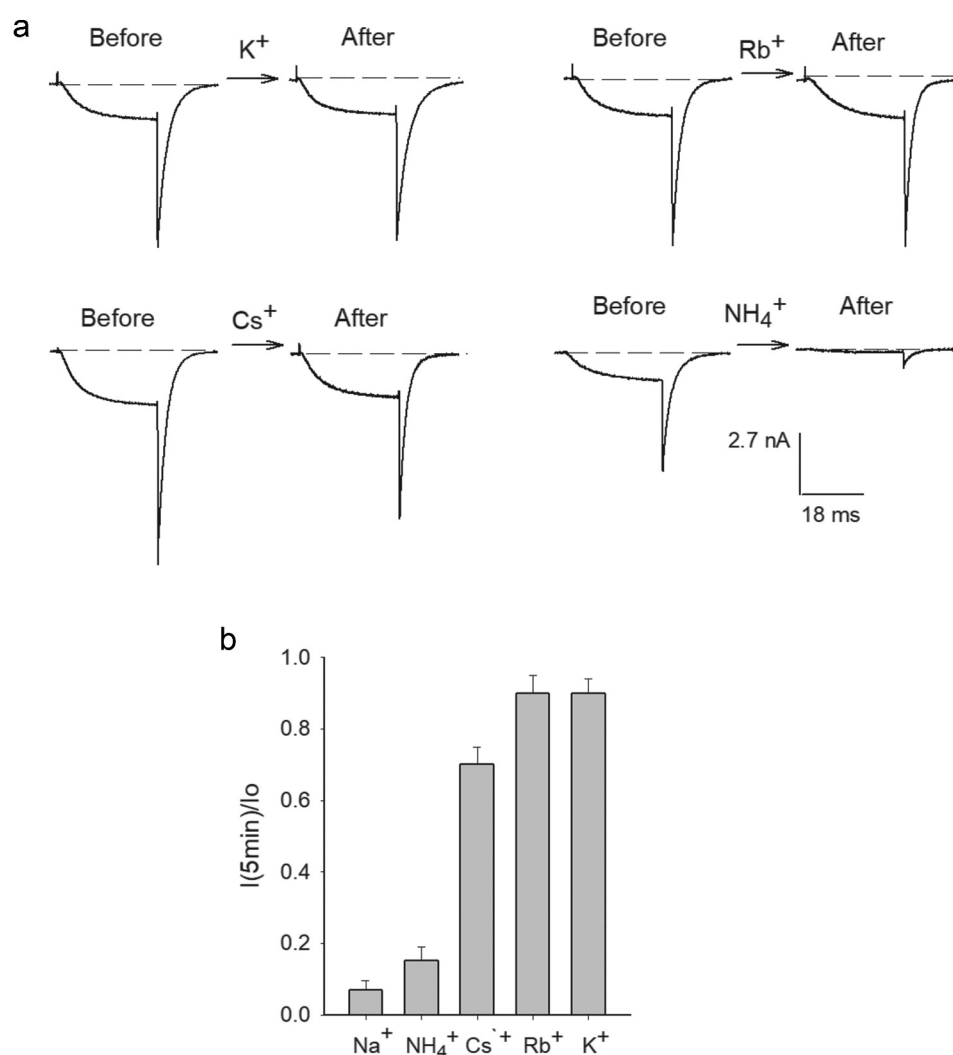


Figure 3. Inhibition of G_K drop by externally added monovalent cations. (a) Representative I_K recorded in $30\text{K}_o/\text{Na}_i$ solutions, before (left traces) and after (right traces) bathing the cells for 5 min in Na_o solution containing the indicated test cation ([test cation] = 5 mM). V_m was kept constant at -80 mV during cells exposure to test solutions. (b) Remaining I_K ($I_K(t=5\text{min})/I_o$) after a 5-min exposure to the indicated solutions. Effects of Rb^+ (0.9 ± 0.05) and K^+ (0.9 ± 0.04) are not statistically different.

blocked by 145 mM TEA_o, at 0 mV. The average dose-response curve of experiments as in A (Figure 4(b)) indicates that TEA_o blocks Shab with a least-squares K_d of 10.8 mM at 0 mV, and 14.5 mM at +60 mV, both obtained by fitting the points with a Michaelis-Menten curve (lines through the points).

The latter is best appreciated in the inset which shows the plot of least-squares K_d vs. V_m. Notice that TEA_o affinity decreases with voltage, as expected. The line is the fit of the points with a standard Woodhull equation [21], with parameters K_d(0 mV) = 10.8 mM, and electrical distance d = 0.12 which agrees with a superficially located TEA_o binding site (see Figure legend). Once the basic parameters of TEA_o block were determined, its effect on G_K stability was studied (Figure 4(c)) following the protocol in (Figure 1(a)), namely: Control I_K was recorded in 30K_o/Na_i solutions (trace labeled 1) and thereafter the cell was superfused for 5 min with 145 mM TEA, 0 K⁺, external solution (indicated by the arrow), finally the cell was superfused back with 30K_o solution, and the state of the channels was tested. The trace in the right panel (labeled 2) shows that TEA_o inhibited G_K drop (compare against Figure 1(a)), but in an extent smaller than that expected considering its blockage affinity (~15% of channels remained active).

After having observed the above result, we considered that it had been reported that mammalian Kv2.1 channels cease to be blocked by TEA_o upon K⁺ removal, and that micromolar amounts of external K⁺ restore block [22] (see Discussion). Therefore, we tested again the effect of TEA_o on G_K drop (Figure 4(d)), but this time adding 0.5 mM K_o⁺ to the test TEA_o solution (0.5 K⁺+145 TEA_o/Na_i). A comparison of control I_K (left panel, labeled 1) against I_K left after bathing the cell for 5 min with 0.5K+TEA_o solution (middle panel, labeled 2) shows that this time TEA_o inhibited G_K drop in an extent (~75%) near to that expected from its apparent block affinity in standard recording conditions.

Finally, to check for the possibility that the increased G_K protection could have been exerted by the co-added 0.5 mM K⁺, immediately after middle I_K was recorded, the cell was superfused for 5 minutes with a 0.5 mM K_o solution lacking

TEA (0.5K_o/Na_i). The trace in the right corner (labeled 3) shows that 0.5 mM K_o⁺ by itself is unable to preserve G_K (see Discussion). These observations are summarized in (Figure 4(e)). Note that 145 mM TEA_o (i.e., TEA_o+0.5K_o) effectively protected G_K (~80%), in near quantitative agreement with its expected extent of block. TEA_o blocks Shab with electrical distance of 0.12, consistent with TEA_o binding right above the selectivity filter as expected [23,24]. Hence, the observations in (Figures 1b, 3 & 4) indicate that (1) placing a suitable ion at the extracellular entry of the pore keeps G_K quite stable, and (2) rule out the possibility that TEA_o inhibition of G_K drop might be due to its trapping of K⁺ ions within the pore (see Discussion).

Na⁺ permeation under low [K⁺] conditions

In addition to its destabilizing effect on G_K, we observed that intracellular hypokalemic conditions also drop the pore selectivity, allowing Na⁺ permeation at negative voltages. This is illustrated by comparing currents evoked by a 0 mV/30 ms pulse in cells bathed in a common Na_o solution, and internal solutions containing either physiological [K⁺] (Na_o/K_i) (Figure 5(a)), or 35 mM [K_i] (Na_o/35K_i, Nernst K⁺ equilibrium potential V_k = -54 mV) (Figures 5(b,c)). In the case of standard Na_o/K_i solutions, at pulse end V_m was stepped to -170 mV to provide a strong driving force for, a possible, Na influx through the channels. Note that, as expected for a typical K⁺ channel, there is not any inward, Na⁺-carried current, as indicated by the arrow. In contrast, recordings carried out in Na_o/35K_i solutions (Figure 5(b)), show a conspicuous inward Na⁺ current at -140 mV (easily seen in the Figure inset which shows tail currents in an expanded scale). Note that at -110 mV current is quite small, indicating that this voltage is near the thermodynamic equilibrium potential of the permeant K⁺ and Na⁺ ions. Accordingly, at -100 mV tail current is outward, and carried only by K⁺ ions (see later). It is important to mention that in order to inhibit the ion conductance drop HP was -120 mV. Thereafter, we seek to determine whether physiological K_o could restore channels selectivity and/or stability. Thus, once the currents in (Figure 5(b))

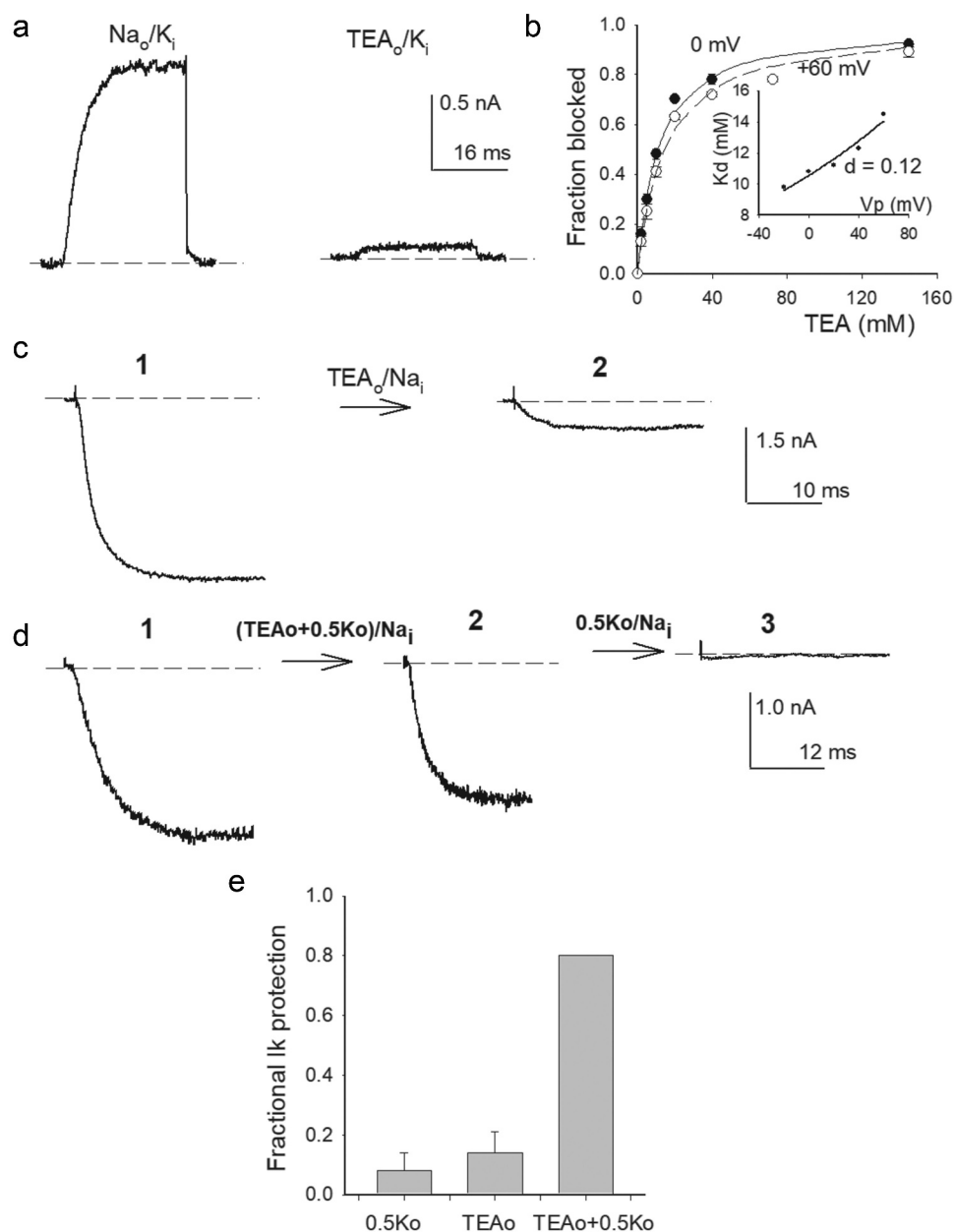


Figure 4. TEA_o block and inhibition of G_K drop. (a) Left panel, control I_K evoked by a 0 mV/30 ms pulse applied from -80 mV in Na_o/K_i solutions. Right panel, I_K recorded upon bathing the same cell with 145 mM TEA_o solution (see Methods), ~80% of I_K was blocked. (b) Fractional TEA_o block vs. [TEA_o]. Fraction blocked = 1 - (I([TEA])/I_o), where I([TEA]) is I_K amplitude in the presence of the indicated [TEA], I_o is the corresponding control I_K. Closed circles: test pulse = 0 mV; open circles: test pulse = +60 mV. The lines are the fit of the points with a Michaelis-Menten equation with K_d(0 mV) = 10.8 mM, or K_d(+60 mV) = 14.5 mM. Inset: K_d vs. V_m. K_ds are the best fit parameters of the corresponding Michaelis-Menten curves. The line is the fit of the points with a Woodhull equation: K_d(V_m) = K_d(0) * exp[zd(F/RT) * V_m]; with parameters d = 0.12, K_d(0 mV) = 10.5 mM, z = +1; F, R, T have their usual meaning. (c) TEA_o inhibition of G_K collapse in 0 K⁺. Left panel: Control I_K evoked by a 0 mV/30 ms pulse, applied from -80 mV, in 30K_o/Na_i solutions (labeled 1). Right panel: I_K left after immersing the cell in, 0 K⁺, TEA_o solution (TEA_o/Na_i) for 5 min, with V_m constant at -80 mV (trace labeled 2, see Methods). (d) TEA_o inhibition of G_K collapse in the presence of 0.5 mM K_o⁺. Left panel: Control I_K recorded as in C (labeled 1). Middle panel: I_K left after superfusing the cell for 5 min with TEA_o solution containing 0.5 mM [K_o⁺], with V_m at -80 mV (labeled 2). Right panel: I_K left after the subsequent exposure of the same cell in 2 to Na_o (0 TEA) solution, containing 0.5 mM [K_o⁺], at -80 mV (labeled 3). (e) Fractional I_K protection after bathing the cells for 5 min in the indicated solutions.

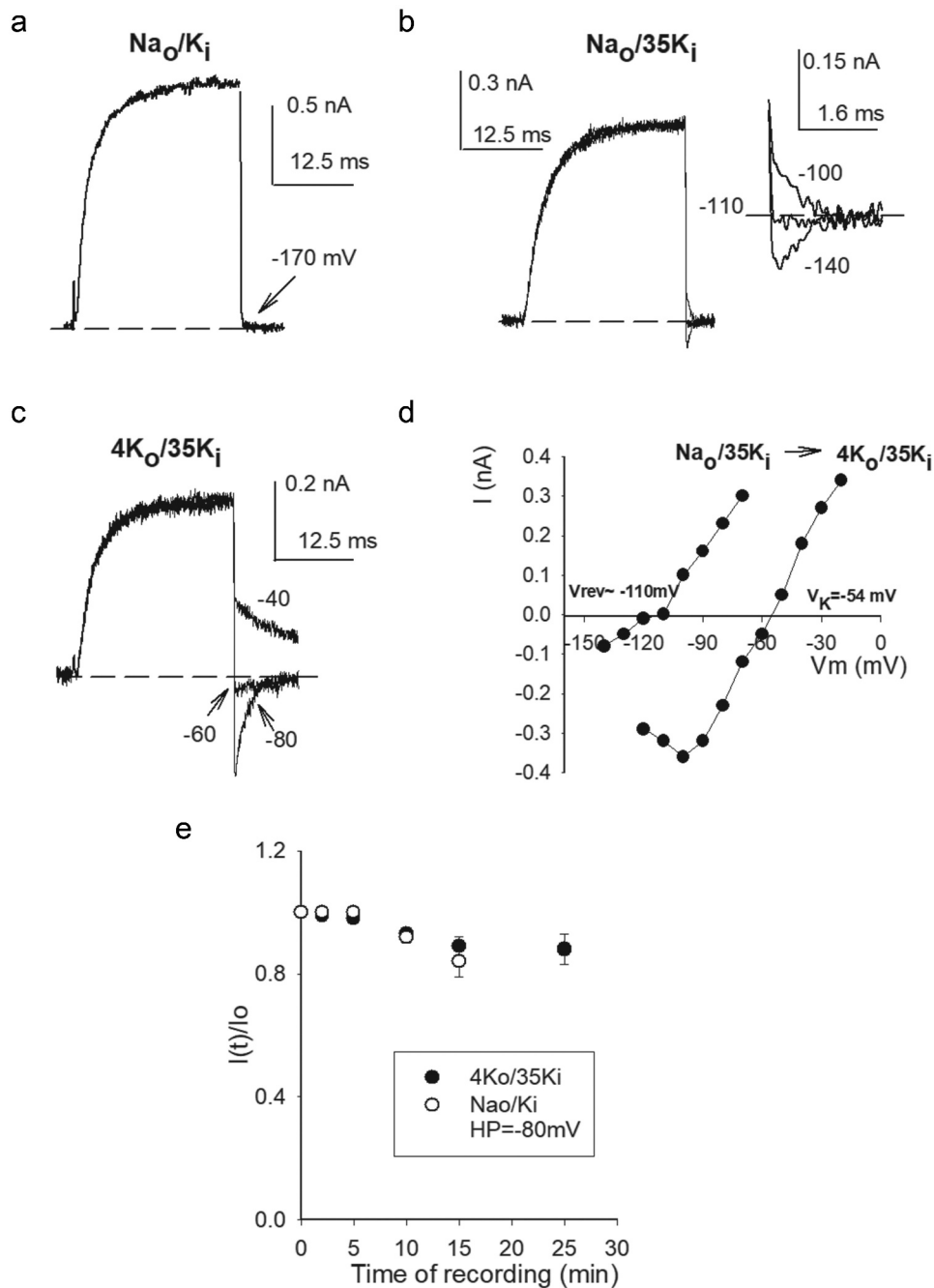


Figure 5. Selectivity and stability in hypokalemic conditions. (a) I_K recorded in standard Na_o/K_i solutions. Current was evoked by a 0 mV/30 ms pulse applied from -80 mV; repolarization potential was -170 mV. There is no inward current at -170 mV (b) Superposed currents recorded in $\text{Na}_o/35\text{K}_i$ solutions in a different cell. Currents were evoked as in A, at pulse end V_m was stepped to the potentials indicated in the inset, which shows tail currents in an expanded scale, HP was -120 mV. Note the small but conspicuous inward Na^+ -carried current. (c) Currents recorded in $4\text{K}_o/35\text{K}_i$ solutions in the same cell as in B. Tail currents V_m are indicated. Notice the shift in current reversal potential as compared to that in B. HP was -120 mV. (d) Instantaneous I-V relationship of the experiments in B & C (see Text). (e) Conductance stability in $4\text{K}_o/35\text{K}_i$ solutions. Note that 4 mM K_o affords G_K stability. Stability in $4\text{K}_o/35\text{K}_i$ solutions turned out to be similar to that in standard Na_o/K_i solutions, HP was -80 mV in both cases.

were recorded the cell was superfused with 4 mM K_o solution. The traces in (Figure 5(c)) ($4\text{K}_o/35\text{K}_i$) illustrate that 4 mM $[\text{K}_o^+]$ restores the K^+ channels characteristic property of excluding Na^+

permeation, as the current now changes direction at the expected Nernst K^+ potential ($V_K = -54$ mV). The above is best seen in (Figure 5 (d)) which shows the instantaneous I-V

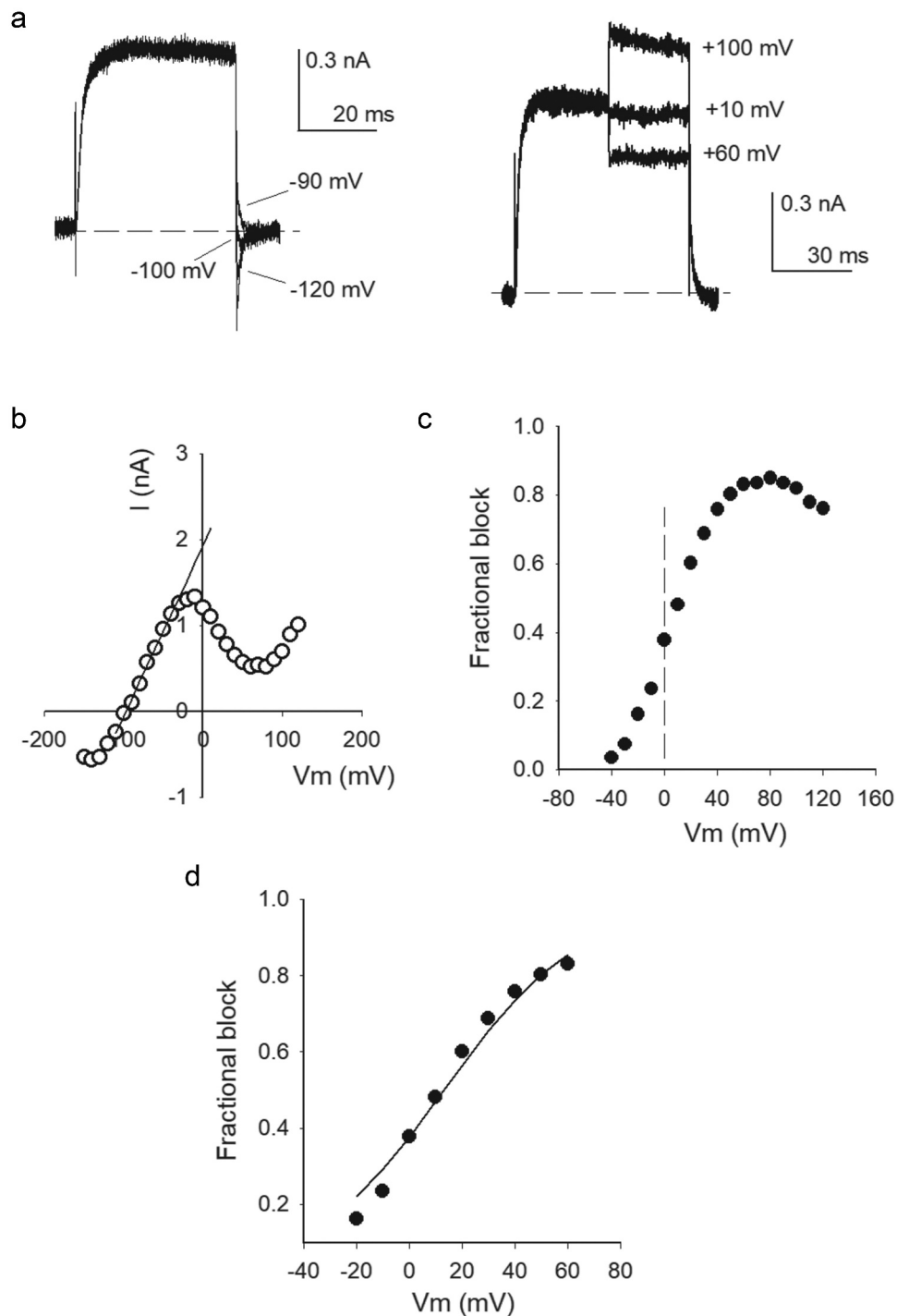


Figure 6. Na⁺ permeation and block in low K⁺ conditions. (a) Left panel: Superposed currents (Na_o/20K_i solutions) evoked by 0 mV/30 ms pulses, at pulse end V_m was repolarized to the indicated potentials. Note the inward Na⁺ current. Right panel: currents recorded in the same cell in A illustrating internal Na⁺ block, and the voltage-driven unblock of the pore (see Text). (b) Instantaneous I-V relationship of the traces in A. (c) Fractional Na_i block vs. V_m. Fractional block was assessed as: $f_b = 1 - (I_o/I_e)$, where I_e is the expected current in the absence of Na_i block, and I_o is the actual, observed, current (see Text). I_e was evaluated from the least-squares line (solid straight line through the points in B) that fits the observed current (I_o) between -80 and -40 mV, where I_o varies linearly with V_m ($r = 0.999$): $I_e = 1.98 + (0.019)V_m$. The vertical dashed line helps to visually separate f_b at negative vs. positive V_m. (d) Fractional Na⁺ block restricted to the voltage range where f_b does not decrease with V_m, data from C. The line is the fit of the points with a Woodhull equation: $K_d(0) \cdot \exp[zd(F/RT) \cdot V_m]$, with $z = +1$, $d = 0.98$, $K_d(0) = 170$ mM.

relationship of the traces in B&C. Note that: V_{rev} ($Na_o/35K_i$) ≈ -110 mV, where V_{rev} is the thermodynamic reversal potential ($<V_{rev} \geq -115 \pm 9$ mV, $n = 5$) (see Figure legend, and below); and that on the other hand, $V_{rev}(4K_o/35K_i) = -55.3$ mV ($<V_{rev} \geq -55.1 \pm 1.5$ mV, $n = 4$). This shows that 4 mM [Ko] halts the anomalous Na^+ conductance.

Although the study of this phenomena falls outside the scope of the present work, notice also that the I-V points with 4 Ko show a conspicuous negative slope at $V_m < -100$ mV, this slope is caused by external Ca^{2+} block of the pore, its dependence on the ion conditions has already been noticed [6,25] (see also Figures 6 & 7). Finally, (Figure 5(e)) shows that, besides halting Na^+ permeation, 4 mM [Ko] keeps G_K stable. It is interesting to also note that, coincidentally, G_K stability in $4K_o/35K_i$ solutions turned out to be similar to that observed with physiological K_i (Na_o/K_i), both measured at the HP of -80 mV.

The above observations show that under hypokalemic (non-zero K^+) conditions G_K is destabilized, and Na^+ permeates through Shab channels at negative voltages. Additionally, notice that the observations collaterally show that a hyperpolarized HP affords G_K stability (see also Figure 2(c)) but, as expected, do not restore selectivity. This supports the notion that conductance selectivity and stability are not strictly coupled parameters of K^+ channels function (see below & Discussion). For completeness, we thereafter assessed Na^+ interaction with the channels at depolarized voltages, with hypokalemic solutions approaching the 0 K^+ limit.

Na^+ block under near 0 K^+ conditions ($[Na^+]$ $[K^+]$ solutions)

It is known that internal Na^+ blocks K^+ channels in a voltage dependent manner; under physiological conditions block develops at positive membrane potentials, while still higher voltages relieve Na^+ block [e.g., 4, 26–30].

Figure 6(a) illustrates the measurement of Na^+ permeation (negative V_m , left panel), and Na^+ block followed by pore unblock (depolarized V_m , right panel), carried out in the same cell, with solutions near the 0 K^+ limit ($Na_o/20K_i$, the lowest $[K_i]$ which allowed us to find cells with measurable

I_K , with reasonable frequency). The currents in (Figure 6(a)) were elicited by a 0 mV pulse (Figure legend), and thereafter V_m was stepped to the indicated potentials; HP was -120 mV to stabilize the ion conductance. The traces in the left show a conspicuous I_{Na} upon membrane repolarization to -120 mV. On the other hand, the traces in the right show that, due to internal Na^+ block, current at $+60$ mV is anomalously smaller than that at $+10$ mV, but that at $+100$ mV current has an amplitude that is expectedly bigger than that at $+60$ mV, illustrating the well-known voltage-promoted unblock of the pore [26,27]. The above is best seen in the instantaneous I-V relationship of the traces in A (Figure 6(b)), notice that: (a) $V_{rev} \approx -100$ mV. In particular, also notice that both the ionic solutions employed and the I-V plot demonstrate that, for $V_m < V_{rev}$ inward current is carried only by Na^+ , and that for V_m positive to but near V_{rev} , outward current is carried only by K^+ ions, which validates the use of the Goldman bi-ionic equation to assess permeability ratios (see later) (the hint of a negative slope at the most negative V_m is due to Ca_o^{++} block) (b) Na^+ block at depolarized V_m becomes apparent at voltages as low as ≈ -20 mV, hence from ~ -10 to $+70$ mV the I-V slope is negative, due to the voltage dependence of Na^+ blockage; (c) at $V_m > +80$ mV the I-V slope is again positive, due to the voltage-promoted unblock of the pore [26,27].

The voltage dependence of Na^+ block of the traces in A is best seen in the fractional Na^+ block (fb) vs. V_m graph (Figure 6(c)). fb was assessed as: $fb = 1 - (I_o/I_e)$, where I_o is the observed current, and I_e is the expected current, that would be obtained in the absence of Na^+ block. I_e was evaluated from the least-squares straight-line (solid line in B) that fits the points between -80 and -40 mV, where current varies linearly with V_m (see Figure legend), as reported [4]. Notice that: (a) Na^+ block becomes apparent from negative V_m (e.g., $f_b \approx 20\%$, at -20 mV). The dashed vertical line serves to point out this feature; (b) Na^+ block is relieved, fb decreases, at $V_m \geq V_{min} \approx +80$ mV, where V_{min} stands for the minimum voltage needed to unblock the pore.

Figure 6(d) shows the fb vs. V_m relationship of the traces in A, restricted to the voltage range where fb slope is not negative. The line is the least-

squares fit of the points with a Woodhull equation (see Figure Legend) with zero-voltage block affinity $K_d(0 \text{ mV}) = 170 \text{ mM}$, and electrical distance $d = 0.95$. The latter value suggests that Na^+ blocks the pore by binding within the selectivity filter itself, as supported by the observations in Figure 5 (see also Figure 7 & Discussion).

The above observations suggest that, in the limit condition of 0 K^+ , internal Na^+ could possibly interact with those channels that manage to randomly open at the resting potential (see Discussion).

Finally, we tested the effect of physiological $[\text{K}_o^+]$ on Na^+ block and permeation. Figure 7(a) compares average I-V s obtained in either $\text{Na}_o/20\text{K}_i$ (as in Figure 6(b)) or $5\text{K}_o/20\text{K}_i$ conditions in 4 different cells. In order to compare both average curves, I-V s were normalized to its mathematical maximal amplitude (i.e., where the slope of the points is zero). The figure also shows the straight lines I_e , as in Figure 6 (Figure legend). Note that: (1) V_{rev} with 5 K_o is shifted to the expected K^+ Nernst potential ($V_K = -35 \text{ mV}$), a shift of $\sim 65 \text{ mV}$ compared to V_{rev} with 0 K_o ; and that (2) with both external solutions (0 & 5 K_o) Na^+ block becomes apparent from negative voltages. Na^+ blockage in 0 vs $5 \text{ mM } [\text{K}_o]$ are best compared in (Figure 7(b)). Block was assessed from the distance of the points to the least squares lines I_e in A, that indicate the expected non-blocked current (see Figure legend). Note that adding 5 K_o increases V_{min} in $\sim 20 \text{ mV}$. The latter is in contrast to the 65 mV shift of V_{rev} . This shows that V_{min} is a parameter comparatively poorly sensitive to $[\text{K}^+]$ across the membrane. As pointed out by Reuter & Stevens (1980) [30], V_{min} is related to the energy barrier, B_{Na} , that has to be overcome for Na^+ to unblock the pore toward the external solution. B_{Na} can be calculated with the equation [30]: $B_{\text{Na}} = F \cdot V_{\text{min}}$, where F is the Faraday constant. According to this relationship, adding $5 \text{ mM } \text{K}_o^+$ increases the energy needed for internal Na^+ to unblock the pore, in an amount equal to $\Delta B_{\text{Na}} = 1.9 \text{ KJ/mol}$. This extra energy likely arises from the presence of a K^+ ion dwelling above the Na^+ blocking site in the pore, with both ions probably located within the selectivity filter. Figure 7(c-d) compare the Na^+ -blockage parameters $K_d(0 \text{ mV})$ and electrical distance d , with

either 0 or 5 K_o , respectively, obtained by fitting the data with a corresponding Woodhull equation, as in (Figure 6(d)). Note that, adding $5 \text{ mM } [\text{K}_o]$, leaves the electrical distance d basically unchanged ($P = 0.911$), suggesting that, even with $5 \text{ mM } [\text{K}_o^+]$ Na^+ is able to bind within the selectivity filter. On the other hand, see that Na^+ affinity at zero voltage, $K_d(0 \text{ mV})$, was increased 1.4 times, yielding a $\Delta \Delta G = 2.8 \text{ J/mol}$. A change in energy much smaller than that required to unblock the pore $\Delta B_{\text{Na}} = 1.9 \text{ KJ/mol}$.

Finally, (Figure 7(e)) presents the relative Na^+ permeability (P_{Na}/P_K) of Shab channels bathed in Na_o solution, as a function of $[\text{K}_i^+]$, obtained from experiments as in (Figures 5–7). P_{Na}/P_K was evaluated by applying the Goldman equation to average thermodynamic current-reversal potentials $\langle V_{\text{rev}} \rangle$, as follows:

$$P_{\text{Na}}/P_K = [\text{K}_i] / \{ [\text{Na}_o] \cdot \exp(-F \cdot \langle V_{\text{rev}} \rangle / RT) - [\text{Na}_i] \}$$
; where F , R , & T have their usual meaning.

See that, as internal K^+ decreases the Na^+ permeability has a non-monotonic variation, first increasing, but thereafter decreasing as $[\text{K}_i]$ approaches 0 , as expected from the conspicuous inward Na^+ currents under hypokalemic non- 0 K^+ conditions, and from the lack of noticeably Na^+ currents either with 0 K^+ across the membrane, or with standard (Na_o/K_i) solutions.

Discussion

Studying Shab channels within the cell membrane environment of cells bathed in 0 K^+ external solution (Na_o), we found that as $[\text{K}_i^+]$ decreases G_K drops at -80 mV in a way suggestive of a transition $[\text{K}_i]$, around which the pore either falls relatively fast into an irreversible non-conducting conformation, or remains comparatively longer in a conducting conformation. This observation qualitatively agrees with studies carried out with isolated KcsA channels, where a transition $[\text{K}^+]$ was suggested, around which two structures are formed, either the so called low (non-conducting) or high K^+ (capable to conduct), crystal structures [12–14]. It is important to note however that in Shab even when G_K is comparatively stable with $120 > [\text{K}_i] \geq 60 \text{ mM}$, the pore structure is

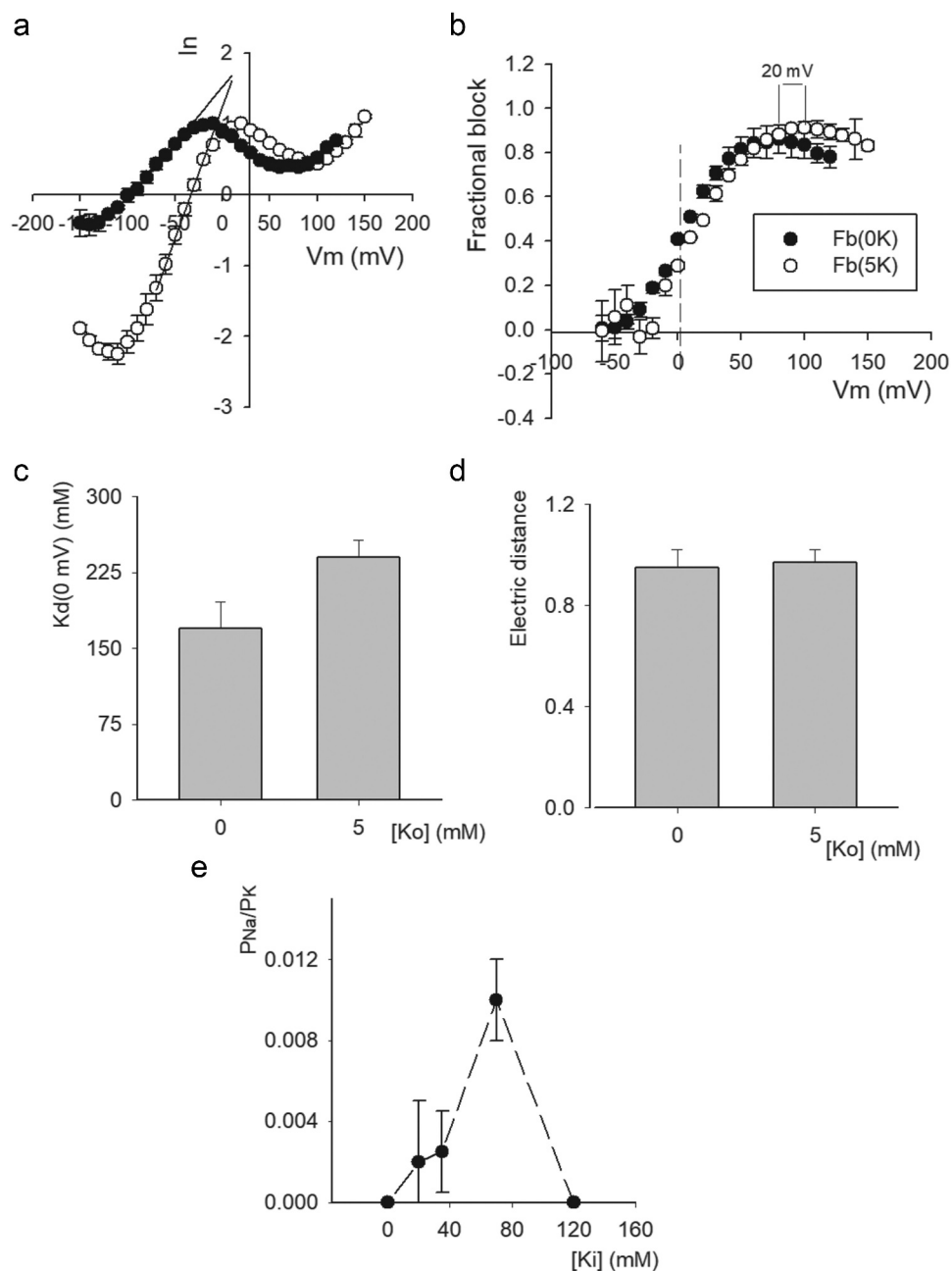


Figure 7. Na⁺ permeation & block with physiological [K⁺]. (a) Average instantaneous I–V relationships recorded either in Na_o/20K_i or 5K_o/20K_i conditions obtained from experiments as in Figure 6A. To allow comparison, currents were normalized to its local maximal value (see Text). (b) Fractional Na_i block vs. V_m. Na_i⁺ block was assessed with the least-squares lines that fit the linear regions of the points at negative V_m, as in Figure 6, namely: 0K_o(–90 to –50 mV): $I_e = 1.52 + 0.016 \cdot V_m$, $r = 0.998$; 5K_o(–70 to –30): $I_e = 1.24 + 0.037 \cdot V_m$, $r = 0.999$. The vertical dashed line serves to visually separate negative from positive voltages. (c) Comparison of 0 voltage affinity, K_d(0 mV), in 0 vs 5 K_o conditions; affinities are statistically different ($P = 0.0634$). (d) Comparison of block electrical distance, d , in 0 vs. 5K_o conditions; values are not statistically different ($P = 0.911$). The parameters K_d(0 mV) & d were obtained by fitting the corresponding fractional block vs V_m relationships with a Woodhull equation, as in Figure 6. (e) P_{Na}/P_K vs. [K_i]. P_{Na}/P_K was evaluated with the Goldman equation (see Text) applied to the corresponding average current reversal-potentials, from experiments as in Figure 5–7. Points are mean ± sem of at least 4 experiments.

nonetheless somehow altered, as evidenced by the anomalous permeation of Na⁺ at negative voltages.

On the other hand, comparison of the effect of non-saturating, nearly mirror, [K⁺] across the

membrane on conductance stability, showed that K⁺ effect is asymmetrical, with external K⁺ being significantly more effective than internal K⁺. This asymmetry could simply be a consequence of the

externally oriented location of the selectivity filter, and/or of the cytoplasmic location of the activation gate, which sets a barrier to K^+ flux [9,31]. It could also obey to a differential stabilizing role of the different K^+ -sites of the pore (see below). Whatever the case, the asymmetric effectiveness of K^+ stands as a physiologically relevant feature of K^+ channels functioning. Regarding the above, we found that the potency with which external cations prevent Shab G_K drop ($K^+ \approx Rb^+ > Cs^+ > NH_4^+ Na^+$) does not match the K^+ channels selectivity sequence. We hypothesize that the G_K protection-sequence may correspond to the selectivity of the particular K^+ -site(s) where G_K is kept stable by externally present suitable ions (see below for TEA). As a reference, it should be mentioned that monovalent ions stabilize the KcsA tetramer with a potency equal to that here reported for Shab [32,33]. Although, on the other hand, in ShakerB, it was found that all permeant ions protect G_K with comparable effectiveness [2]. The structural basis of this difference is puzzling since both channels share the conserved signature-sequence of K^+ channels.

In addition to permeant ions, we observed that the, non-permeant, TEA ion protects G_K from the external side of the membrane. This result agrees with observations showing that TEA_o inhibits G_K drop of Shaker in 0 K^+ [2]. In the case of Shab, but not of Shaker, in order for TEA_o to efficiently protect G_K , it was necessary to add a low (0.5 mM) $[K_o^+]$, a K^+ concentration which by itself does not inhibit G_K drop. K^+ was added to the TEA_o solution after considering that mammalian Kv2.1 channels are blocked by external TEA with a K_d of 5 mM [34,35], but cease to be blocked by this cation in the absence of K^+ . The latter occurs because a lysine residue (K326) in the outer vestibule of Kv2.1 pore seems to reorient in a way that fully hinders TEA_o binding in the absence of K^+ [22,34]. Shab also has lysine at the equivalent Kv2.1 position, which along with the small extent of TEA protection of G_K observed in the absence of external K^+ , suggests that this residue may undergo a similar reorientation in 0 K^+ in both channels.

Interestingly, internal TEA also ceases to block Kv2.1 in the absence of K^+ , this shows that the

conformational channel triggered from the lack of K^+ extends from the external vestibule to the central cavity of Kv2.1. Pore block by both internal and external TEA are equally restored by the low micromolar amounts of K^+ which also block Na^+ permeation through Kv2.1 [34].

In the case of Shab, and the squid K channel, pore block in Na_o/K_i solutions, by either internal quinidine, or TEA, promotes the irreversible collapse of G_K [36,37]. This effect arises because cation-blockers (like quinidine and TEA), upon binding within the central cavity, electrostatically repel the stabilizing K^+ ions dwelling in the selectivity filter, leading to a virtual 0 K^+ condition where G_K irreversibly collapses.

As mentioned before, besides abolishing TEA block it was also observed a flux of Na^+ through Kv2.1 in the absence of K^+ [22,34], however, we are not aware of any studies regarding the K^+ -dependent stability of Kv2.1 channels.

TEA_o inhibition of Shab G_K drop, along with the significant asymmetry of K^+ effectiveness to maintain G_K stable, suggest that the outermost pore site (s1/s2), and/or a conformational rearrangement of the external pore vestibule, have a relevant role regarding G_K stability (see also [38]).

Na⁺ permeation and blockage with hypokalemic solutions

In addition to destabilize G_K , hypokalemic (non-zero K^+) solutions allow the passage of Na^+ through Shab. Na^+ permeation in the absence of K^+ has been observed in other K^+ channels, as for example Shaker [38–40], Kv2.1 [22], and Kv1.5 [41]. However, this has not been observed in all K^+ channels, as for example Kv10.1 (unpublished observations). Here we showed that, adding low, physiological $[K_o]$ restores both selectivity and G_K stability.

As $[K_i]$ decreases the relative P_{Na}/P_K ratio reaches a peak and thereafter decreases, as $[K_i]$ approaches 0. This behavior underlines the lack of a conspicuous Na^+ -current in the limit of 0 K^+ . Thus, although K^+ prevents Na^+ permeation, likely through a Koshland induce-fit mechanism [22,42], a minimal $[K^+]$ is nonetheless required to keep a pore conductive-structure

that, paradoxically, allows Na^+ permeation. The non-monotonic $P_{\text{Na}}/P_{\text{K}}$ variation contrasts with the progressive (monotonic, although non-uniform) G_{K} stability decrement as $[\text{K}_i^+]$ decreases. This difference, along with the differential effect of hyperpolarized V_m on G_{K} stability and selectivity, further supports the notion that: pore stability and selectivity, although clearly related, are not strictly coupled parameters (see also [6,8]).

With solutions that approach the 0 K^+ limit ($\text{Na}_o/20\text{K}_i$), we observed that Na^+ block becomes apparent from negative potentials, with a blockage electrical-distance near to one. These observations: (a) reinforce the notion that Na^+ ions are indeed capable to bind within the selectivity filter itself; (b) suggest that in the limit of 0 K^+ across the membrane Na^+ may possibly interact with those channels that manage to randomly open at the resting potential, somehow catalyzing G_{K} collapse. This hypothesis may explain at least part of the stabilizing effect afforded by hyperpolarized potentials, since hyperpolarized V_m values further prevent channel opening, hence they should also decrease Na^+ block of randomly open channels (for an extensive discussion of the role of V_m in G_{K} stability see [7,8,38]).

Summary of Shab G_{K} stability and selectivity under hypokalemic solutions

The observations herein reported are summarized in cartoon form in (Figure 8). The upper left panel (labeled as state 1) depicts the stable and K^+ selective selectivity filter of the pore, as seen in high K^+ (saturating) conditions ([9]), (a condition seemingly reached in either Na_o/K_i , or $30\text{K}_o/\text{Na}_i$ solutions). There are two K ions at a time in the filter (blue spheres) ([9]).

Upon partly replacing K^+ with Na^+ , channels transit to an unstable “transition” state (labeled 2), having an undermined G_{K} stability and selectivity, at a rate a_1 that depends on both X_{K} and V_m , as indicated. In the unstable state 2 the pore allows Na^+ permeation at negative V_m , hence a Na^+ ion is depicted in the selectivity filter as a small red sphere, and G_{K} spontaneously drifts to zero (state 3), depending on V_m and X_{K} . The unstable state 2 can be only partly reverted, and the

channels regain stability and selectivity, by actively adding K^+ , indicated by a^{-1} . However, the fraction of already lost G_{K} (transition 2 \rightarrow 3), cannot be recovered.

The non-conducting and irreversible state 3 can be reached directly, and comparatively faster, from the stable high K^+ condition (1 \rightarrow 3) upon full removal of K^+ , at a rate r that depends on V_m . As a hypothesis we depicted the stable (irreversible) state 3 as containing a Na^+ ion(s) within the selectivity filter, but without being capable of conducting any type of ions. Finally, it must be commented that the 2TM KcsA tetramer loses its thermal stability in the absence of K^+ [32,33], this possible final step, that would follow state 3, has not yet been demonstrated in 6TM K^+ channels. It is important to point out that in state 2 Shab allows the passage of Na^+ from the open (non-inactivated) state (as evident in the traces in Figures 5–6). This differs from Shaker channels which allow the transient passage of Na^+ from the C-type inactivated state, before collapsing (see Figure 1 of Hoshi & Armstrong, 2013 [38], and references therein cited), and in this case in a reversible manner [2]. This difference may somehow be related to the fact that Shab slow inactivation is not a C-type inactivation [43], see below.

Physiological consequences of the K^+ -dependent stability of K^+ channels

Although the number of K^+ channels whose possible K^+ -dependent stability has been studied is still small, conditions in which G_{K} loss by hypokalemia may be related to a pathological condition had already been reported, for example: As mentioned before, intracellular channel blockers of clinical use, like the antiarrhythmic quinidine may cause the G_{K} collapse of delayed rectifier K^+ channels, like Shab or the squid channel, under, extracellular, hypokalemic conditions [36,37]. Within the organism the latter condition can be elicited by a number of factors, including vomiting [44]. The drop of G_{K} being a risky, potential side effect, of intracellularly-acting cationic drugs [36,37]. Regarding heart physiology, it has been reported that with a low serum $[\text{K}^+]$ the HERG K channel, a key participant of the repolarization phase of the cardiac action

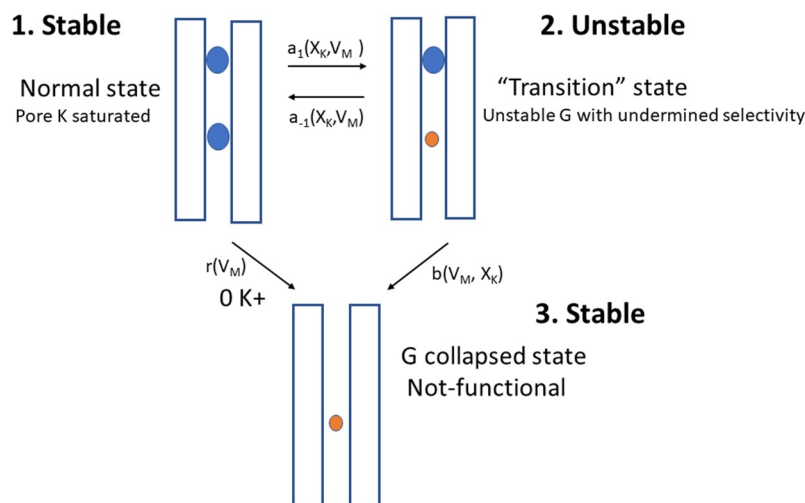


Figure 8. Summary of Shab K⁺ channel behavior as a function of [K⁺] across the membrane. Upper left image (state 1): Under saturating [K⁺] the selectivity filter has 2 K⁺ ions at a time (blue spheres, Doyle et al [9]), Gk is stable & selective, irrespective of V_m. Upper right panel (state 2): Upon K⁺ replacement by equimolar amounts of Na⁺ ions the channel visits a "transition", meaning unstable, state (1->2, right panel), where Gk falls with a rate that depends on X_K & V_m (K⁺ molar fraction) and V_m. In this unstable state the pore conformation allows Na⁺ permeation from the open, non-inactivated, state (a Na⁺ ion is indicated in the pore by the small red sphere), depending on V_m. Negative HP or K⁺ addition restore stability (indicated by the left pointing arrow), although: the already lost G is not recovered (i.e., arrows connecting states 1 & 2 do not indicate a truly reversible transition). Lower panel (state 3): With 0 K⁺ across the membrane (1->3) the channel readily falls into the stable (i.e., irreversible) not conducting state 3; alternatively, under hypokalemic (non-zero K⁺ conditions) the channels sink although more slowly into state 3 (2->3) depending on X_{K+}. In both cases (1->3 and 2->3) the rate of Gk collapse depends on V_m. In the nonconducting 0 K⁺ state 3 the pore may possibly contain Na⁺ ion(s), but it is unable to conduct any type of ion.

potential, and hence of cardiac rhythm, cease to conduct K⁺ by falling in a reversible non-conducting state, a condition that can lead to sudden cardiac death [45,46]. Thereafter, non-conducting HERG channels are removed from the cardiac muscle membrane, so when the normal serum [K⁺] is reestablished by hemostatic mechanisms, cardiac muscles have a transiently lower HERG channels density, with a risk of developing arrhythmias [45,46]. HERG channels fall into this non-conducting state in a gating-independent fashion, in a manner seemingly similar to that of Kv1.4 channels [45–47]. These examples show that more studies are still needed to assess the possible K⁺-dependent stability, and selectivity, of K⁺ channels subtypes. Finally, for the sake of completeness, it should be mentioned that increases in extracellular K⁺, like those that transiently occur in the confined extracellular medium of neurons upon firing action potentials, produce the well-known acceleration of recovery from ball-and-chain inactivation, and slow down the entry into C-type inactivation ([38] and references therein cited). Shab presents a non-C type

slow inactivation, increases of external K⁺ accelerate the entry [43] and slow down the recovery from slow inactivation [48]. These examples show that increases in external [K⁺] dynamically change the amount of K⁺ channels available to repolarize the cells.

Acknowledgments

This work was supported by DGAPA-PAPIIT IN219918 and IN215221. The authors declare that they have no conflict of interest

Disclosure statement

No potential conflict of interest was reported by the author(s).

Funding

This work was supported by the supported by UNAM-PAPIIT IN219918 and IN215221.

References

- [1] Almers W, Armstrong CM. Survival of K⁺ permeability and gating currents in squid axons perfused with K⁺-free media. *J Gen Physiol.* **1980**;75:61–78.
- [2] Gómez-Lagunas F, Shaker B K⁺ conductance in Na⁺ solutions lacking K⁺ ions: a remarkably stable non-conducting state produced by membrane depolarizations. *J Physiol.* **1997**;499:3–15.
- [3] Ambriz-Rivas M, Islas LD, Gómez-Lagunas F. K⁺-dependent stability and ion conduction of Shab K⁺ channels: a comparison with Shaker channels. *Pflügers Arch.* **2005**;450:255–261.
- [4] Gómez-Lagunas F. Na⁺ interaction with the pore of Shaker B K⁺ channels: zero and low K⁺ conditions. *J Gen Physiol.* **2001**;118:639–648.
- [5] Melishchuk A, Loboda A, Armstrong CM. Loss of Shaker K channel conductance in 0 K⁺ solutions: role of the voltage sensor. *Biophys J.* **1998**;75:1828–1835.
- [6] Carrillo E, Pacheco L, Balleza D, et al. K⁺-dependent selectivity and external Ca²⁺ block of Shab K⁺ channels. *PlosOne.* **2015**;10:e0120431.
- [7] Gómez-Lagunas F. Stability of the Shab K⁺ channel conductance in 0 K⁺ solutions: the role of the membrane potential. *Biophys J.* **2007**;93:4197–4208.
- [8] Loboda A, Melishchuk A, Armstrong CM. Dilated and defunct K channels in the absence of K⁺. *Biophys J.* **2001**;80:2704–2714.
- [9] Doyle DA, Cabral JM, Pfuetzner A, et al. The structure of the potassium channel: molecular basis of K⁺ conduction and selectivity. *Science.* **1998**;280:69–76.
- [10] Heginbotham L, Lu Z, Abramson T, et al. Mutations in the K⁺ channel signature sequence. *Biophys J.* **1994**;66:1061–1067.
- [11] Zhou Y, Morais-Cabral JH, Kaufman A, et al. Chemistry of ion coordination and hydration revealed by a K⁺ channel-Fab complex at 2.0 Å resolution. *Nature.* **2001**;414:43–48.
- [12] Lockless SW, Zhou M, MacKinnon R. Structural and thermodynamic properties of selective ion binding in a K⁺ channel. *PLoS Biol.* **2007**;5:1079–1088.
- [13] Renart ML, Barrera FN, Molina ML, et al. Effects of conducting and blocking ions on the structure and stability of the potassium channel KcsA. *J Biol Chem.* **2006**;281:29905–29915.
- [14] Zhou Y, MacKinnon R. The occupancy of ions in the K⁺ selectivity filter: charge balance and coupling of ion binding to a protein conformational change underlie high conduction rates. *J Mol Biol.* **2003**;333:965–975.
- [15] Block BM, Jones SW. Delayed rectifier current of bullfrog sympathetic neurons: ion-ion competition, asymmetrical block and effects of ions on gating. *J Gen Physiol.* **1997**;499:403–416.
- [16] Zhu Y, Ikeda SR. Anomalous permeation of Na through a putative K channel in rat superior cervical ganglion neurons. *J Physiol.* **1993**;468:441–461.
- [17] Butler A, Wei A, Salkoff L, Shal, Shab and Shaw: three genes encoding potassium channels in *Drosophila*. *Nucleic Acids Res.* **1990**;18:2173–2174.20.
- [18] Islas LD, Sigworth FJ. Voltage sensitivity and gating charge in Shaker and Shab family potassium channels. *J Gen Physiol.* **1999**;114:723–742.
- [19] Neher E. Correction for liquid junction potentials in patch clamp experiments. *Methods Enzymol.* **1992**;207:123–131.
- [20] Stewart BA, Atwood HL, Renger JJ, et al. Improved stability of *Drosophila* larval neuromuscular preparations in hemolymph-like physiological solutions. *J Comp: Physiol A.* **1994**;175:179–191.
- [21] Woodhull AM. Ion blockage of sodium channels in nerve. *J Gen Physiol.* **1973**;61:687–708.
- [22] Ikeda SR, Korn SJ. Influence of permeating ions on potassium channel block by external tetraethylammonium. *J Physiol.* **1995**;486:267–272.
- [23] Heginbotham L, MacKinnon R. The aromatic binding site for tetraethylammonium ion on potassium channels. *Neuron.* **1992**;8:483–491.26.
- [24] Crouzy S, Berneche S, Roux B. Extracellular blockade of K⁺ channels by TEA: results from molecular simulations of the KcsA channel. *J Gen Physiol.* **2001**;118:207–217.
- [25] Gómez-Lagunas F, Melishchuk A, Armstrong CM. Block of Shaker potassium channels by external calcium ions. *Proc Natl Acad Sci USA.* **2003**;100:347–351.
- [26] Bezanilla F, Armstrong CM. Negative conductance caused by the entry of sodium and cesium ions into the potassium channels of squid axons. *J Gen Physiol.* **1972**;60:588–608.
- [27] French RJ, Wells JB. Sodium ions as blocking agents and charge carriers in the potassium channel of the squid giant axon. *J Gen Physiol.* **1977**;70:707–724.
- [28] Yellen G. Ion permeation and blockade in Ca²⁺--activated K⁺ channels of bovine chromaffin cells. *J Gen Physiol.* **1984**;84:157–186.
- [29] Nimegean CM, Miller C. Na⁺ block and permeation in a K⁺ channel of known structure. *J Gen Physiol.* **2002**;120:323–335.
- [30] Reuter H, Stevens CF. Ion conductance and ion selectivity of potassium channels in snail neurons. *J Membr Biol.* **1980**;57:103–118.
- [31] Armstrong CM. Interaction of tetraethylammonium ion derivatives with the potassium channels of giant axons. *J Gen Physiol.* **1971**;58:413.
- [32] Krishnan MN, Trombley P, Moczydlowski EG. Thermal stability of the KcsA channel tetramer: cation interactions and the conserved threonine residue at the innermost site (S4) of the KcsA selectivity filter. *Biochemistry.* **2008**;47:5354–5367.
- [33] Krishnan MN, Bingham JP, Lee SH, et al. Functional role and affinity of inorganic cations in stabilizing the tetrameric structure of the KcsA K⁺ channel. *J Gen Physiol.* **2005**;126:271–283.

- [34] Immke D, Wood M, Kiss L, et al. Potassium dependent changes in the conformation of the Kv2.1 potassium channel pore. *J Gen Physiol.* **1999**;113:819–836.
- [35] Tagliatela M, Van Dongen AMJ, Drewe JA, et al. Patterns of internal and external tetraethylammonium block of four homologous K⁺ channels. *Mol Pharmacol.* **1991**;40:299–307.
- [36] Khodakhah K, Melishchuk A, Armstrong C. Killing channels with TEA⁺. *Proc Natl Acad Sci USA.* **1997**;94:13335–13338.
- [37] Gomez-Lagunas F. Quinidine interaction with Shab K⁺ channels. Pore block and irreversible collapse of the K⁺ conductance. *J. Physiol.* **2010**;588(15):2691–2706.
- [38] Hoshi T, Armstrong CM. C-type inactivation of voltage-gated K⁺ channels: pore constriction or dilation? *J Gen Physiol.* **2013**;141:151–156.
- [39] Ogielska EM, Aldrich RW. A mutation in S6 of Shaker potassium channels decreases K⁺ affinity of an ion binding site revealing ion-ion interactions in the pore. *J Gen Physiol.* **1998**;112:243–257.
- [40] Starkus JG, Heinemann S, Rayner M. Voltage dependence of slow inactivation in Shaker potassium channels results from changes in relative K⁺ and Na⁺ permeabilities. *J Gen Physiol.* **2000**;115:107–122.
- [41] Zhuren W, Xue Z, Fedida D. Regulation of transient Na⁺ conductance by intra- and extracellular K⁺ in the human delayed rectifier K⁺ channel Kv1.5. *J Physiol.* **2000**;523:575–591.
- [42] Segel IH. *Enzyme kinetics: behavior and analysis of rapid equilibrium and steady state enzyme systems.* New York: Wiley; **1975**.
- [43] Carrillo E, Arias-Olguin I, Islas LD, et al. Shab K⁺ channel slow inactivation. *Channels.* **2013**;7:1–12.
- [44] Goodman & Gilman's *The Pharmacological Basis of Therapeutics.* Molinoff PB, Ruddon RW eds. 13th edition (2017). Mc Graw Hill. New York, USA.
- [45] Guo J, Massaeli H, Xu J, et al. Extracellular K⁺ concentration controls cell surface density of IKr in rabbit hearts and of the HERG channel in human cell lines. *J Clin Invest.* **2009**;119:2745–2757.
- [46] Massaeli H, Guo J, Xu J. Extracellular K⁺ is a prerequisite for the function and plasma membrane stability of HERG channels. *Circ Res.* **2010**;106:1072–1082.47.
- [47] Pardo LA, Heinemann SH, Terlau H, et al. Extracellular K⁺ specifically modulates a rat brain K⁺ channel. *Proc Natl Acad Sci USA.* **1992**;89:2466–2470.
- [48] Arias-Olgin II, Carrillo E, Islas LD, et al. Recovery from slow inactivation of Shab K⁺ channels. *Channels.* **2013**;7(3):1–4.